IEEE Access
Multidisciplinary | Rapid Review | Open Access Journal

Received 22 November 2022, accepted 3 December 2022, date of publication 8 December 2022,
date of current version 16 December 2022.

Digital Object Identifier 10.1109/ACCESS.2022.3227801

RESEARCH ARTICLE

Batteryless Machine-Type Communications With Average Channel State Information Energy Beamforming

RAFAELA SCACIOTA[1,2], (Student Member, IEEE), ONEL L. ALCARAZ LÓPEZ[2], (Member, IEEE), GLAUBER BRANTE[1], (Senior Member, IEEE), RICHARD DEMO SOUZA[3], (Senior Member, IEEE), ANDRÉ A. MARIANO[4], (Senior Member, IEEE), AND GUILHERME LUIZ MORITZ[1], (Member, IEEE)

[1]Graduate Program in Electrical and Computer Engineering, Federal University of Technology—Paraná (UTFPR), Curitiba 80230-901, Brazil
[2]Centre for Wireless Communications (CWC), University of Oulu, 90570 Oulu, Finland
[3]Departament of Electrical and Electronics Engineering, Federal University of Santa Catarina (UFSC), Florianópolis 88040-900, Brazil
[4]Department of Electrical Engineering, Federal University of Paraná (UFPR), Curitiba 81531-980, Brazil

Corresponding author: Rafaela Scaciota (rafaelas@alunos.utfpr.edu.br)

This work was supported in part by CAPES, Brazil, under Finance Code 001, Grant CNPq 402378/2021-0, Grant CNPq 305021/2021-4, Grant CNPq 307226/2021-2, and Grant CNPq 309796/2020-2; in part by the Finnish Foundation for Technology Promotion and Academy of Finland under Grant 348515 and Grant 346208 (6G Flagship); and in part by the EC Research Innovation Action under the H2020 Program under the Project HPC-EUROPA3 under Grant INFRAIA-2016-1-730897. Rafaela Scaciota gratefully acknowledges the support of Onel L. Alcaraz López, the computer resources and technical support provided by CWC.

ABSTRACT Machine-type communication (MTC) is a key component in 5G and beyond wireless networks, enabling important applications oriented to the industry. In such environments, the limited lifetime of battery-powered solutions becomes a relevant reliability issue. In this paper, we consider a sensor node powered wirelessly by a dedicated multi-antenna power beacon (PB). The harvested energy is directly used by the sensor to power its transceiver and send information to a destination node without storing it in a battery, which would demand non-negligible charging time and potentially compromise the MTC operation. Also, we leverage a packet replication mechanism during information transmission from the sensor to the destination in order to improve the system reliability. We derive the incident power statistics and the outage probability assuming Rician fading channels and only average channel state information at the PB. Then, we define an optimization problem aiming to minimize the energy required by the PB by properly tuning the number of replicated packets and the harvesting time. Results show the existence of an optimal harvesting time as well as an optimal number of replications for a given number of PB antennas, enabling batteryless MTC applications.

INDEX TERMS Machine-type communication, batteryless, power beacon, packet replication, average channel state information.

I. INTRODUCTION

The manufacturing industry is facing a digital transformation driven by the exponential growth of intelligent devices, such as sensors, robots, 3D printing, *etc.* The future of manufacturing tends towards connecting industry components wirelessly, delivering data more flexibly and adaptively. Such a revolution, known as Industry 4.0, shares concepts with the Internet of Things (IoT), focusing on interconnectivity, automation, machine learning, and real-time data transmission. According to Ericsson [1], 39 billion IoT connections are foreseen for 2026, with around 27.5 billion of them related to the industry.

Machine-type communication (MTC) is one of the key components to integrate communications and manufacturing requirements, evolving industrial applications [2]. Here,

The associate editor coordinating the review of this manuscript and approving it for publication was Adao Silva.

packet replication (PR) is a promising solution as it allows increasing the system reliability without needing a feedback channel. For instance, PR is used in [3] to deal with multipath fading by prioritizing uncorrelated paths to replicate packets. The scheme provides resilience to multipath fading and benefits delay-sensitive applications. In [4], the authors compare automatic repeat request (ARQ) and PR strategies in industrial networks, investigating the trade-offs of energy and bandwidth versus reliability and availability. Notice that the implementation of ARQ implies waiting for an acknowledgment message before retransmitting a packet, while PR relies on pro-actively transmitting multiple replicas of the same packet without waiting for a feedback, at the cost of increasing the required spectral efficiency to meet latency constraints. The PR approach proposed in [4] reduces the packet error rate by approximately six times, at the cost of increasing the energy consumption by around 10% compared to ARQ.

Notice that satisfying MTC service requirements may be power consuming due to the unreliable nature of the wireless medium. Taking the power consumption into consideration, the authors in [5] reduce the communication energy budget by making reliability/latency constraints more flexible. A dynamic allocation algorithm is provided in order to detect when such constraints can be relaxed, aiming for reduced energy consumption. The authors in [6] propose a low-latency distributed scheduling function to minimize the latency while providing high reliability. The process reorganizes the slotted frame into smaller blocks so that each transmitter selects a set of blocks depending on its hop distance from the router, better distributing retransmissions. Then, to save energy, nodes can turn off their radio as soon as their packets are correctly acknowledged. Also, the authors in [7] evaluate the benefits of improving communication reliability by combining PR with modulation diversity using multiple IEEE 802.15.4g transmission modes. Such a combination is shown to increase the system reliability while maintaining the same energy consumption.

Common to [5], [6], and [7] is the effort to save energy from battery-powered MTC devices. Nevertheless, as pointed out by [8], the evolution of industrial manufacturing employing battery-operated sensors today may become a maintenance problem in the future. This is motivated by the need to replace batteries across thousands of devices constantly. In this regard, wireless energy transfer (WET) technology has emerged as a suitable option for charging low-power devices, such as industrial sensors. Specifically, WET enables radio frequency (RF) to direct current (DC) power conversion without physical connections, while enabling small-form factor implementations and natively supporting multi-user charging [9], [10], [11].

WET is a growing research topic in the literature, with recent approaches found, *e.g.*, in [12], [13], [14], and [15]. The authors in [12] study wireless powered communications where multiple access points collaborate using distributed energy beamforming in the downlink, so that energy harvesting (EH) devices can transmit in the uplink. Results show significant gains in terms of coverage and transmission probabilities when multiple access points collaborate for WET. A wireless-powered backscatter communication network is considered in [13], where a transmitter harvests energy from a dedicated RF source. Then, a Dinkelbach-based algorithm is formulated to maximize the energy efficiency by jointly optimizing the time allocation, the reflection coefficient, and the transmit power of the source.

However, perfect instantaneous channel state information (CSI) is usually considered in the design of energy beamforming vectors, thus becoming inefficient, or unfeasible, due to the time and energy consumption during CSI acquisition. Moving to more practical approaches, the work in [14] studies the relationship between the EH rate and the data rate with imperfect instantaneous CSI. By formulating the energy beamforming design as a max-min optimization problem, the proposed scheme achieves more than 90% of the data rate obtained with perfect CSI. Assuming that instantaneous CSI is not available, the authors in [15] study the optimal deployment of power beacons (PBs) to satisfy an energy outage constraint. The proposed solution provides a framework in which neither CSI nor devices' locations are known, so that PBs' positions are optimized to maximize the minimum average RF energy.

Another important implication of WET that is often neglected in the literature is the time required to charge a battery/supercapacitor. An EH device uses a rectenna to convert RF into a DC power source, and the recovered DC power is stored in a battery for higher power low duty-cycle operations. That is the basis of harvest-then-transmit schemes, so that WET and wireless information transfer (WIT) phases occur in sequence. However, storing energy in a battery or supercapacitor demands time at least in the order of seconds due to the resistor-capacitor (RC) time constant of the circuit [16], [17], which is unfeasible for some industrial applications. Such charging time is often overlooked by the WET literature, although it plays a crucial role in time-critical applications.

In this work, we focus on a short distance scenario, typical of the WET-enabled solutions emerging in the market. As an example, the PowerSpot® RF Wireless Power Development Kit [18] enables battery-free wireless sensor applications in a charging distance of up to a few meters. In this context, we consider a batteryless industrial sensor node and a nearby dedicated multi-antenna PB, which is employed in order to supply energy to the sensor with high reliability. The recovered DC power at the sensor node powers the transceiver directly by means of the power management unit (PMU) [19], without storing it in a battery. The implication is that WET and WIT phases must occur simultaneously in this case. In the WIT phase, the sensor node transmits information to a destination node that performs automation tasks, so the communication must occur within a maximum time deadline and with a target outage probability constraint. Our approach yields the following contributions:

- We derive the incident power statistics and the outage probability assuming Rician fading channels and average CSI (A-CSI) beamforming at the PB.
- We define an optimization problem to determine the number of replicated packets in the WIT phase and the charging time in the WET phase, to minimize the energy required from the PB. We exploit the convexity and strictly monotonic properties of the problem to solve it iteratively.
- We show the existence of an optimal harvesting time and an optimal number of replications for a given number of antennas at the PB. Remarkably, the optimal values for the practical A-CSI scheme are only slightly larger than those of the ideal full CSI (F-CSI) beamforming.

Notation: Boldface lowercase letters denote column vectors, while boldface uppercase letters denote matrices. $\mathbf{I}$ denotes the identity matrix. $||\cdot||$, $|\cdot|$, $(\cdot)^H$ and $(\cdot)^T$ stand for the Euclidean norm, absolute value, Hermitian transpose and transpose operations, respectively. $\mathbb{E}_x[\cdot]$ denotes the statistical expectation over the variable x, and j is the imaginary unit, *i.e.*, $j = \sqrt{-1}$. $\mathbb{C}$ is the set of complex numbers, $\mathbf{x} \sim \mathcal{CN}(\mathbf{m}, \mathbf{R})$ is a circularly-symmetric complex Gaussian random vector with mean vector $\mathbf{m}$ and covariance matrix $\mathbf{R}$, and $x \sim \mathcal{N}(a, b)$ is a Gaussian random variable with mean a and variance b. $F_{\mathbf{A}}(x)$ stands for the cumulative distribution function (CDF) of the random variable $\mathbf{A}$ and $f_{\mathbf{A}}(x)$ represents its probability density function (PDF). Moreover, $Q_\nu(\cdot,\cdot)$ is the Generalized order ν Marcum Q-function and $I_0(\cdot)$ is the Bessel function of the first kind. Additionally, for convenience, the rest of the acronyms and symbols adopted in this work are summarized in Tables 1 and 2, respectively.

TABLE 1. List of acronyms adopted in this work.

Acronym	Meaning
ARQ	Automatic Repeat reQuest
A-CSI	Average Channel State Information
BLE	Bluetooth Low Energy
CSI	Channel State Information
CDF	Cumulative Distribution Function
DC	Direct Current
EH	Energy Harvesting
F-CSI	Full Channel State Information
i.i.d.	Independent and Identically Distributed
IoT	Internet-of-Things
LOS	Line Of Sight
MRC	Maximal Ratio Combining
MRT	Maximum Ratio Transmission
MTC	Machine-Type Communication
PA	Power Amplifier
PB	Power Beacon
PDF	Probability Distribution Function
PMU	Power Management Unit
PSD	Power Spectral Density
PR	Packet Replication
RC	Resistor-Capacitor
RF	Radio Frequency
SNR	Signal-to-Noise Ratio
ULA	Uniform Linear Array
WET	Wireless Energy Transfer
WIT	Wireless Information Transfer

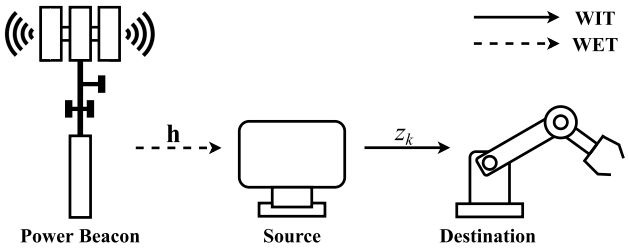

FIGURE 1. System diagram with WET and WIT phases.

II. SYSTEM MODEL

We assume the scenario in Figure 1, consisting of a WET link to power the source using a PB, and a WIT link to transmit data from the source to the destination. Furthermore, WET and WIT phases occur *simultaneously* during a time T_i, for $i \in \{\text{A-CSI, F-CSI}\}$. In the WET link, the PB is equipped with a uniform linear array (ULA) of M antennas and the source uses a single rectenna to harvest energy, so that the WET channel vector is denoted as $\mathbf{h} \in \mathbb{C}^{M\times 1}$. The PB employs an A-CSI precoder [20], while the recovered DC power at the source is immediately used by the transceiver through the PMU. In the WIT link, the source node employs a PR mechanism, transmitting K_i replicas of the same packet during the time T_i to increase the system reliability. Both source and destination are assumed single-antenna. Figure 1 shows the WIT channel for the k-th replication, denoted by $z_k \in \mathbb{C}$. Finally, we assume that the communication between source and destination must occur within a maximum time deadline $T_{\max}$ and with a target outage probability constraint $\mathcal{O}^\star$.

A. CHANNEL MODELS

1) WET LINK

The channel between the PB and the source is subject to Rician fading with line of sight (LOS) factor κ_{wet} and coherence time T_c. The channel vector of the WET link can be written as [21] and [20]

$$\mathbf{h} = \sqrt{\beta_{\text{wet}}}(\bar{\mathbf{h}} + \tilde{\mathbf{h}}) \in \mathbb{C}^{M\times 1}, \tag{1}$$

where $\bar{\mathbf{h}}$ is the deterministic LOS component, and $\tilde{\mathbf{h}}$ is the zero-mean scattering (random) component with covariance $\mathbf{R} = \mathbb{E}\left[\tilde{\mathbf{h}}\tilde{\mathbf{h}}^H\right]$. Then, we have that [20], [21]

$$\bar{\mathbf{h}} = \sqrt{\frac{\kappa_{\text{wet}}}{1+\kappa_{\text{wet}}}}\, e^{j\varphi_0}\,[1, e^{j\psi_1}, \cdots, e^{j\psi_{M-1}}]^T, \tag{2}$$

$$\tilde{\mathbf{h}} \sim \sqrt{\frac{1}{1+\kappa_{\text{wet}}}}\mathcal{CN}(\mathbf{0}, \mathbf{R}), \tag{3}$$

where ψ_t, $t \in \{1, \cdots, M-1\}$, is the mean phase shift of the $(t+1)$-th array element with respect to the first

TABLE 2. List of symbols adopted in this work.

Symbol	Meaning
M	Number of antennas at the PB
K_i	Number of replicas of the same packet
T_i	Harvesting/Transmission time
R_i	Spectral efficiency
i	Precoding scheme $i \in \{\text{A-CSI}, \text{F-CSI}\}$
N	Number of bits per packet
c	Speed of light
B	System bandwidth
$\mathbf{h}$	Channel vector of the WET link
$\bar{\mathbf{h}}$, $\tilde{\mathbf{h}}$	LOS/Scattering of the WET link
κ_{wet}, κ_{wit}	LOS factor of the WET/WIT link
ψ_t	Mean phase shift of the $(t+1)$-th array element w.r.t. the first PB antenna
φ_0	Initial phase shift of the PB antenna array
θ	Azimuth angle to the boresight of the PB antenna array
β_{wet}, β_{wit}	Average power gains
f_{wet}, f_{wit}	Carrier frequencies
d_{wet}, d_{wit}	Distances
α_{wet}, α_{wit}	Path-loss exponents
z_k	Channel of the k-th replication in WIT
$\bar{z}$ / $\tilde{z}_k$	LOS/Scattering of the WIT link
ϕ	Mean phase shift of the source's antenna
T_{c}	WET/WIT channel coherence time
$\mathbf{w}_i$	MRT precoder
$\mathcal{P}_i$	RF power harvested by the source
P_{b}	Transmit power of the PB
$\mathcal{G}(x)$	Nonlinear rectenna EH function
$\mathcal{W}$	EH saturation level
c_0	Nonlinear EH rate w.r.t. the input power
c_1	Minimum turn-on voltage of the EH circuit
ξ_i	Harvesting efficiency
η	Drain efficiency of the PA
P_{circ}	Transceiver fixed power consumption
P_i^{tx}	Transmit power
P_i^{total}	Total power consumption
$P_{\max}^{\text{tx}}$	Maximal transmission power
γ_i	Instantaneous SNR
γ_0	SNR threshold for correct decoding
N_{f}	Noise figure
N_0	Noise PSD
$\lvert z_\Sigma \rvert^2$	Equivalent channel due to the MRC of K_i
$\mathcal{O}_i$	Outage probability
$\mathcal{O}^\star$	Target outage probability
$\mathcal{E}_i^\star$	Energy required by the PB
$K_{\max}$	Maximal number of replicas
$T_{\max}$	Maximum time deadline
$R_{\max}$	Maximum spectral efficiency

antenna, and φ_0 accounts for an initial phase shift. Assuming half-wavelength equally spaced antenna elements, it follows that $\psi_t = -t\,\pi\,\sin\theta$, where $\theta \in [0, 2\pi]$ is the azimuth angle relative to the boresight of the transmitting antenna array. Moreover, the average power gain in the WET link is

$$\beta_{\text{wet}} = \frac{c^2}{(16\pi^2 f_{\text{wet}}^2 d_{\text{wet}}^{\alpha_{\text{wet}}})}, \tag{4}$$

where c is the speed of light, f_{wet} is the carrier frequency in the WET link, d_{wet} is the PB-source distance, and α_{wet} is the path-loss exponent.

2) WIT LINK

The source node establishes WIT to the destination through a channel subject to Rician fading with LOS factor κ_{wit}. In addition, the same coherence time T_{c} is assumed, since WET and WIT occur simultaneously. Both nodes are assumed single-antenna. In addition, we assume different channel realizations for each of the K_i replications. Such model is representative of frequency hopping, where replications occur in different channel realizations.[1] Thus, for the k-th replication, $k \in [1, K_i]$, we have

$$z_k = \sqrt{\beta_{\text{wit}}}\,(\bar{z} + \tilde{z}_k) \in \mathbb{C}, \tag{5}$$

where $\bar{z}$ is the deterministic (LOS) component, and $\tilde{z}_k$ is the zero-mean scattering (random) component, so that

$$\bar{z} = \sqrt{\frac{\kappa_{\text{wit}}}{1+\kappa_{\text{wit}}}}\, e^{j\phi}, \tag{6}$$

$$\tilde{z}_k \sim \sqrt{\frac{1}{1+\kappa_{\text{wit}}}}\mathcal{CN}(0,1), \tag{7}$$

where ϕ is the mean phase shift. Moreover, β_{wit} is the average power gain, which is given by

$$\beta_{\text{wit}} = \frac{c^2}{16\,\pi^2 f_{\text{wit}}^2 d_{\text{wit}}^{\alpha_{\text{wit}}}}, \tag{8}$$

where f_{wit} is the carrier frequency in the WIT link, d_{wit} is the distance, and α_{wit} is the path-loss exponent.

B. PACKET REPLICATION

In the WIT link, the source node employs PR. Thus, it transmits K_i packets with the same information to the destination in order to increase the reliability against packet losses. The total number of bits per packet is denoted by N. Then, the destination employs maximal ratio combining (MRC) in order to combine all replicas of the same packet. Therefore, the normalized rate, or spectral efficiency, for the scheme $i \in \{\text{A-CSI, F-CSI}\}$ is

$$R_i = \frac{K_i N}{B\,T_i}, \tag{9}$$

where B is the system bandwidth. Notice that the replicas are transmitted during the time T_i, so that increasing K_i implies a higher spectral efficiency R_i to meet the delay constraints. In addition, the outage probability depends on the quality of

[1] For instance, in Bluetooth low energy transceivers channel hopping occurs by default within the 2.4 GHz ISM band, using a 37 channel pseudorandom hopping pattern [22].

the WIT link and on the energy provided by the WET link, which are detailed in Section IV.

III. INCIDENT POWER STATISTICS

We statistically characterize the incident RF power at the source node during the WET phase. We assume A-CSI precoder following [20]. Such beamforming design does not require instantaneous CSI acquisition, thus, avoiding frequent energy-costly feedback/signaling processes. Note that this is a practical approach for MTC applications since it may be very hard (if possible) to acquire instantaneous CSI for these applications. In addition, as a benchmark, we also consider an F-CSI scheme, where perfect instantaneous CSI of the PB-source link is ideally available at the PB. In a general form, assuming a precoder $\mathbf{w}_i$, $i \in \{\text{A-CSI, F-CSI}\}$, the RF power harvested by the source is

$$\mathcal{P}_i = |\mathbf{w}_i^H \mathbf{h}|^2. \tag{10}$$

A. AVERAGE CSI (A-CSI) BEAMFORMING

In order to use only average CSI, we observe that

$$\mathbb{E}[\mathbf{h}] = \sqrt{\beta_{\text{wet}}}\,\bar{\mathbf{h}}, \tag{11}$$

thus, the maximum ratio transmission (MRT) precoder with A-CSI is [20]

$$\mathbf{w}_{\text{A-CSI}} = \frac{\sqrt{P_{\text{b}}}\,\bar{\mathbf{h}}}{||\bar{\mathbf{h}}||}, \tag{12}$$

where P_{b} is the transmit power of the PB. Therefore, substituting (12) into (10) yields

$$\begin{aligned}\mathcal{P}_{\text{A-CSI}} &= \left|\sqrt{P_{\text{b}}}\frac{\bar{\mathbf{h}}^H}{||\bar{\mathbf{h}}||}\mathbf{h}\right|^2 \\ &= \beta_{\text{wet}} P_{\text{b}} \left|||\bar{\mathbf{h}}|| + \frac{\bar{\mathbf{h}}^H\tilde{\mathbf{h}}}{||\bar{\mathbf{h}}||}\right|^2 \\ &= \beta_{\text{wet}} P_{\text{b}} |\delta|^2. \end{aligned} \tag{13}$$

Here, $\bar{\mathbf{h}}^H\tilde{\mathbf{h}} \sim \mathcal{CN}\left(\mathbf{0}, \bar{\mathbf{h}}^H\mathbf{R}\bar{\mathbf{h}}\right)$, thus,

$$\delta = ||\bar{\mathbf{h}}|| + \frac{\bar{\mathbf{h}}^H\tilde{\mathbf{h}}}{||\bar{\mathbf{h}}||} \sim \mathcal{CN}\left(||\bar{\mathbf{h}}||, \frac{\bar{\mathbf{h}}^H\mathbf{R}\bar{\mathbf{h}}}{||\bar{\mathbf{h}}||^2}\right). \tag{14}$$

Moreover, we can decompose δ as

$$\delta = \frac{\sqrt{\bar{\mathbf{h}}^H\mathbf{R}\bar{\mathbf{h}}}}{\sqrt{2}\,||\bar{\mathbf{h}}||}\left(\delta_{\mathcal{R}} + j\delta_{\mathcal{I}}\right), \tag{15}$$

where

$$\delta_{\mathcal{R}} \sim \mathcal{N}\left(\frac{\sqrt{2}\,||\bar{\mathbf{h}}||^2}{\sqrt{\bar{\mathbf{h}}^H\mathbf{R}\bar{\mathbf{h}}}}, 1\right), \tag{16}$$

$$\delta_{\mathcal{I}} \sim \mathcal{N}(0, 1). \tag{17}$$

As a consequence, $\frac{2||\bar{\mathbf{h}}||^2}{\bar{\mathbf{h}}^H\mathbf{R}\bar{\mathbf{h}}}|\delta|^2 = \delta_{\mathcal{R}}^2 + \delta_{\mathcal{I}}^2$ follows a non-central chi-squared distribution with $k = 2$ degrees of freedom, and non-centrality parameter

$$\lambda = \frac{2||\bar{\mathbf{h}}||^4}{\bar{\mathbf{h}}^H\mathbf{R}\bar{\mathbf{h}}}. \tag{18}$$

Given the above, the CDF of $\mathcal{P}_{\text{A-CSI}}$ is [23]

$$F_{\mathcal{P}_{\text{A-CSI}}}(x) = 1 - Q_1\left(\text{a}, \text{b}\sqrt{x}\right), \tag{19}$$

where $Q_\nu(\cdot,\cdot)$ is the generalized Marcum Q-function of order ν, $\text{a} = \sqrt{\frac{2}{\bar{\mathbf{h}}^H\mathbf{R}\bar{\mathbf{h}}}}\,||\bar{\mathbf{h}}||^2$ and $\text{b} = \sqrt{\frac{2}{P_{\text{b}}\beta_{\text{wet}}\bar{\mathbf{h}}^H\mathbf{R}\bar{\mathbf{h}}}}\,||\bar{\mathbf{h}}||$. In addition, assuming i.i.d. Rician fading channels[2] we have $\mathbf{R} = \frac{1}{1+\kappa_{\text{wet}}}\mathbf{I}$ [20], [21], so that

$$\bar{\mathbf{h}}^H\mathbf{R}\bar{\mathbf{h}} = \frac{M\kappa_{\text{wet}}}{(1+\kappa_{\text{wet}})^2}. \tag{20}$$

As a consequence,

$$\text{a} = \sqrt{2\,\kappa_{\text{wet}}\,M}, \tag{21}$$

$$\text{b} = \sqrt{\frac{2(1+\kappa_{\text{wet}})}{P_{\text{b}}\,\beta_{\text{wet}}}}. \tag{22}$$

Furthermore, we can obtain the PDF of the incident RF power as the derivative of (19), so that

$$f_{\mathcal{P}_{\text{A-CSI}}}(x) = \frac{1}{2}e^{\frac{-(\text{a}^2+x\,\text{b}^2)}{2}}\text{b}^2 I_0(\text{a}\,\text{b}\sqrt{x}), \tag{23}$$

where $I_0(\cdot)$ is the modified Bessel function of the first kind.

Let us remark that average CSI of the WET link at the PB could be obtained by an initial setup of the source node, and updated periodically by exchanging pilot symbols.

B. FULL CSI (F-CSI) BEAMFORMING

In this case, $\mathbf{h}$ is assumed perfectly known; thus, the MRT precoder is [20]

$$\mathbf{w}_{\text{F-CSI}} = \frac{\sqrt{P_{\text{b}}}\,\mathbf{h}}{||\mathbf{h}||}, \tag{24}$$

which substituted in (10) yields

$$\mathcal{P}_{\text{F-CSI}} = \left|\sqrt{P_{\text{b}}}\frac{\mathbf{h}^H}{||\mathbf{h}||}\mathbf{h}\right|^2 = \beta_{\text{wet}}P_{\text{b}}||\mathbf{h}||^2. \tag{25}$$

Note that $\mathcal{P}_{\text{F-CSI}}$ is known since we assume F-CSI. However, let us remark that F-CSI beamforming is the ideal solution, but rather unrealistic. That is because perfect knowledge of $\mathbf{h}$ at the PB would require frequent control signaling from the source node to the PB, consuming additional energy and time resources, which are very limited in our scenario. As a consequence, F-CSI is employed in this work only as a performance benchmark for A-CSI, while the latter does not require instantaneous CSI acquisition.

IV. ENERGY AND RELIABILITY ANALYSIS

Notice that the system reliability is affected by the performance of both links. A poor WET channel will decrease the energy availability at the source, impacting the received signal-to-noise ratio (SNR) at the destination during WIT. Meanwhile, a poor WIT channel will directly affect the communication between the source and destination.

[2]The analysis presented here is valid for any channel model, not only for Rician channels. Our choice for the Rician fading channels is to provide a flexible characterization of many practical scenarios, since the severity of the fading can be adjusted through κ_{wet}.

A. ENERGY HARVESTING

Herein, we discuss the electronics of the source node, which impacts both EH and power consumption. First, let us discuss the nonlinear model of the rectenna, which describes the saturation of the output DC power given a large RF input power due to the diode breakdown. Such modeling is circuit-specific and obtained via curve fitting based on measured data. Here, we follow the non-linear function in [19] in order to model the total energy harvested by the rectenna, as

$$\mathcal{G}(x) = \frac{\mathcal{W}(1 - e^{-c_0 x})}{1 + e^{-c_0(x - c_1)}}, \tag{26}$$

with $\mathcal{W}$ denoting the saturation level, *i.e.*, the maximal DC power produced by the EH circuit when the RF input is excessively large, c_0 reflects the nonlinear harvesting rate with respect to the input power, while c_1 determines the minimum turn-on voltage of the EH circuit. Then, for a given incident RF power $\mathcal{P}_i$ at the source, the non-linear function in (26) defines a harvesting efficiency

$$\xi_i = \frac{\mathcal{G}(\mathcal{P}_i)}{\mathcal{P}_i}. \tag{27}$$

B. TRANSCEIVER MODEL

Regarding the WIT circuitry, the power consumption of low-power transceivers is usually modeled as a linear function encompassing the drain efficiency η of the power amplifier (PA), and an additional fixed power consumption P_{circ} associated with other circuit elements of the transceiver [24]. Therefore, to produce a transmit power P_i^{tx}, the transceiver consumes

$$P_i^{\text{total}} = \frac{P_i^{\text{tx}}}{\eta} + P_{\text{circ}}. \tag{28}$$

Assuming that all energy harvested by the rectenna is employed by the transceiver, we have that $P_i^{\text{total}} = \mathcal{G}(\mathcal{P}_i)$, where $\mathcal{P}_i$ is the RF input power at the rectenna when the PB employs the precoder $i \in \{\text{A-CSI, F-CSI}\}$. Thus, the transmit power is

$$P_i^{\text{tx}} = \min\left\{\max\left\{0,\ \eta\left(\mathcal{G}(\mathcal{P}_i) - P_{\text{circ}}\right)\right\}, P_{\max}^{\text{tx}}\right\}, \tag{29}$$

in which the max operation comes from the fact that $\mathcal{P}_i \geq \mathcal{G}^{-1}(P_{\text{circ}})$ must be harvested in order to output $P_i^{\text{tx}} \geq 0$, while the min operation constraints the transmission power to a maximum $P_{\max}^{\text{tx}}$.

C. OUTAGE PROBABILITY

An outage occurs when the instantaneous SNR at the destination γ_i, for $i \in \{\text{A-CSI, F-CSI}\}$, falls below the SNR threshold γ_0 after K replications. Assuming the Shannon limit and spectral efficiency of R_i bits/s/Hz, we set $\gamma_0 = 2^{R_i} - 1$ [25].[3] Meanwhile

$$\gamma_i = \frac{P_i^{\text{tx}}\,\beta_{\text{wit}}\,|z_\Sigma|^2}{N_{\text{f}} N_0 B}, \tag{30}$$

where N_{f} is the noise figure, N_0 is the noise power spectral density (PSD), and $|z_\Sigma|^2 = \sum_{k=1}^{K_i} |z_k|^2$ due to the MRC of the K_i replicas, whose CDF can be written as [23]

$$F_{|z_\Sigma|^2}(x) = 1 - Q_{K_i}\left(\sqrt{2K_i\kappa_{\text{wit}}}, \sqrt{2(1+\kappa_{\text{wit}})x}\right). \tag{31}$$

Thus, the outage probability can be written as

$$\mathcal{O}_i = \Pr\left(\gamma_i < \gamma_0\right) = \Pr\left(|z_\Sigma|^2 < \frac{\gamma_0 N_{\text{f}} N_0 B}{P_i^{\text{tx}}\,\beta_{\text{wit}}}\right). \tag{32}$$

Notice that the Shannon limit approximates very well the average error probability in the finite blocklength regime for the scenario of this paper. As shown in [26], the approximation error in Rician fading can be very small depending on the size of the codeword and LOS factor of the channel. In the scenario considered in this work, the approximation error using the outage probability is smaller than 1.6%.

1) AVERAGE CSI

When only average CSI is available, $\mathcal{P}_{\text{A-CSI}}$ is a random variable and we can exploit the statistical characterization given in Section III to write the overall outage probability. Then, it can be obtained as the average of the incident RF power over the CDF of $|z_\Sigma|^2$, so that

$$\begin{aligned}\mathcal{O}_{\text{A-CSI}} &= \mathbb{E}_{\mathcal{P}_{\text{A-CSI}}}\left[F_{|z_\Sigma|^2}\left(\frac{\gamma_0 N_{\text{f}} N_0 B}{P_i^{\text{tx}}\,\beta_{\text{wit}}}\right)\right] \\ &= \int_{L_1}^{L_2} F_{|z_\Sigma|^2}\left(\frac{\gamma_0 N_{\text{f}} N_0 B}{\eta\left(\mathcal{G}(x) - P_{\text{circ}}\right)\beta_{\text{wit}}}\right) f_{\mathcal{P}_{\text{A-CSI}}}(x)\ \mathrm{d}x \\ &\quad + F_{|z_\Sigma|^2}\left(\frac{\gamma_0 N_{\text{f}} N_0 B}{P_{\max}^{\text{tx}}\,\beta_{\text{wit}}}\right)\int_{L_2}^{\infty} f_{\mathcal{P}_{\text{A-CSI}}}(x)\ \mathrm{d}x,\end{aligned} \tag{33}$$

where L_1 and L_2 are established based on (29), so that to output $0 \leq P_{\text{A-CSI}}^{\text{tx}} \leq P_{\max}^{\text{tx}}$ the source node must harvest $P_{\text{circ}} \leq \mathcal{G}(\mathcal{P}_{\text{A-CSI}}) \leq (P_{\max}^{\text{tx}}\eta^{-1} + P_{\text{circ}})$. Therefore, the first integral considers $\mathcal{P}_{\text{A-CSI}}$ ranging from $L_1 = \mathcal{G}^{-1}(P_{\text{circ}})$ to $L_2 = \mathcal{G}^{-1}(P_{\max}^{\text{tx}}\eta^{-1} + P_{\text{circ}})$, with the transmission power given by $P_{\text{A-CSI}}^{\text{tx}} = \eta\left(\mathcal{G}(\mathcal{P}_{\text{A-CSI}}) - P_{\text{circ}}\right)$. The second integral ranges from L_2 to ∞, which stands for the case of the transmission power saturated at $P_{\text{A-CSI}}^{\text{tx}} = P_{\max}^{\text{tx}}$.

2) FULL CSI

Here, $\mathcal{P}_{\text{F-CSI}}$ is known,[4] thus, the outage probability for the F-CSI scheme can be obtained as (31)

$$\begin{aligned}&\mathcal{O}_{\text{F-CSI}} \\ &= F_{|z_\Sigma|^2}\left(\frac{\gamma_0 N_{\text{f}} N_0 B}{P_{\text{F-CSI}}^{\text{tx}}\,\beta_{\text{wit}}}\right) \\ &= 1 - Q_{K_i}\left(\sqrt{2K_i\kappa_{\text{wit}}}, \sqrt{\frac{2\gamma_0 N_{\text{f}} N_0 B(1+\kappa_{\text{wit}})}{\eta\ \left(\mathcal{G}(\mathcal{P}_{\text{F-CSI}}) - P_{\text{circ}}\right)\beta_{\text{wit}}}}\right).\end{aligned} \tag{34}$$

[3] We have omitted the index i in γ_0 in order to lighten the notation, but $i \in \{\text{A-CSI, F-CSI}\}$ can be easily inferred from the context.

[4] Let us remark that the transmit power used by the source node when the F-CSI precoder is employed at the PB is also limited to $P_{\max}^{\text{tx}}$.

D. PROBLEM FORMULATION

Our goal is to configure K_i and T_i, for $i \in \{\text{A-CSI, F-CSI}\}$, in order to minimize the energy required by the PB, so as to meet a target reliability constraint $\mathcal{O}^\star$. This optimization problem can be formulated as

$$\underset{K_i,T_i}{\text{minimize}} \quad \mathcal{E}_i = P_\text{b}\, T_i \tag{35a}$$
$$\text{s.t.} \quad \mathcal{O}_i \leq \mathcal{O}^\star, \tag{35b}$$
$$T_i \leq T_\text{max}, \tag{35c}$$
$$R_i \leq R_\text{max}. \tag{35d}$$

Observe that since P_b is fixed, the energy-minimization problem is also a latency-minimization problem, *i.e.*, T_i should be as small as possible in order to meet (35b). However, due to the mathematical complexity of the outage probabilities, it is not possible to obtain a closed-form expression to solve the optimization problem. Nevertheless, notice that the outage probability of the A-CSI beamforming in (33) is impacted by $T_\text{A-CSI}$ and $K_\text{A-CSI}$ only in the CDF of $|z_\Sigma|^2$, defined in (31) in terms of the generalized Marcum Q-function. For the F-CSI beamforming, the outage probability in (34) is also written using the generalized Marcum Q-function.

The impact of T_i is observed only in the second argument of $Q_{K_i}(\cdot,\cdot)$, which depends on γ_0 (a function of the transmission rate $R_i = \frac{N K_i}{B T_i}$). By its turn, K_i defines the order of $Q_{K_i}(\cdot,\cdot)$ and impacts both its arguments. Notice that K_i is restricted to integer values and it also impacts the transmission rate. Thus, increasing K_i will be beneficial in order to meet the target $\mathcal{O}^\star$, but it will demand higher energy from the PB so that the source node can transmit at higher rates. As a consequence, practical values for K_i need to be limited to a given K_max.

Furthermore, as pointed out by [27], the Marcum Q-function is convex and strictly monotonic with respect to both arguments when the order (K_i in our case) is fixed. The convexity and strictly monotonic properties of $Q_{K_i}(.,.)$ allow us to transform the inequality constraint in (35b) into an equality in order to save resources. As a consequence, for a given $k \in [1, K_\text{max}]$, we can redefine the bivariate optimization problem in (35a) into

$$\underset{T_i}{\text{minimize}} \quad \mathcal{E}_i = P_\text{b}\, T_i \tag{36a}$$
$$\text{s.t.} \quad \mathcal{O}_i = \mathcal{O}^\star, \tag{36b}$$
$$T_i \leq T_\text{max}, \tag{36c}$$
$$R_i \leq R_\text{max}. \tag{36d}$$

Such a problem is equivalent to finding T_i that yields $\mathcal{O}_i = \mathcal{O}^\star$, which can be solved through numerical methods that narrow the range of values in an interval, as the golden-section search algorithm with parabolic interpolation. The advantage of the golden-section search technique combined with parabolic interpolation, compared to approaches based on the Newton's method, for example, is faster convergence without the need for differentiation [28]. Let us remark that the optimization in (36a) is solved during the setup of the source node. Then, as the scenario considered here has no mobility, the optimization needs only to be updated if the topology changes, yielding negligible complexity to the system operation.

Algorithm 1: Proposed Minimization Algorithm

```
   Input: T_max, K_max
1  Initialize: T_i^⋆ = ∞, K_i^⋆ = 0;
2  forall k ∈ [1, K_max] do
3      Find T_i that solves O_i = O^⋆;
4      if (T_i ≤ T_max)&(R_i ≤ R_max) then
5          if (T_i < T_i^⋆) then
6              T_i^⋆ ← T_i;
7              K_i^⋆ ← k;
8          else
9              End algorithm;
               Output: T_i^⋆, K_i^⋆
10         end
11     end
12 end
```

Algorithm 1 summarizes our proposed approach, in which we define a maximal number of replicas K_max and a maximum time deadline T_max, typical of MTC applications. Then, for each $k \in [1, K_\text{max}]$ we first find T_i that yields $\mathcal{O}_i = \mathcal{O}^\star$. However, notice that solutions with small k may not meet the reliability constraint $\mathcal{O}^\star$ within the time deadline T_max. Thus, if $T_i > T_\text{max}$ the condition in line 4 ensures that these solutions are not taken into account. On the other hand, if $T_i \leq T_\text{max}$ the algorithm runs until T_i decreases when k increases, *i.e.*, the situation that increasing the number of replicas is beneficial in order to meet $\mathcal{O}^\star$, but not compromised by the higher energy demand from the PB. Another important condition in line 4 is with respect to the spectral efficiency of the source node. High k or small T_i may yield impractical values for R_i, which is thus limited to R_max in our solution.

V. NUMERICAL RESULTS

In this section, we present numerical results to illustrate our analysis. The default parameters for simulations are listed in Table 3, unless stated otherwise. For the WET link, we follow a scenario typical of the PowerSpot® RF Wireless Power Development Kit [18], which enables 915 MHz energy transfer up to a maximal charging distance of 6 m. In addition, the non-linear EH function at the sensor node follows [19]. In the WIT link, the energy consumption is representative of a Bluetooth low energy (BLE) transceiver as in [29], while the MTC constraints are representative of a mobile automation scenario with $\mathcal{O}^\star = 10^{-6}$ and $T_\text{max} = 10$ ms [30].

First, Figure 2 illustrates at the top the non-linear energy harvesting function $\mathcal{G}(\mathcal{P}_i)$ versus the incident power $\mathcal{P}_i$, given by (26), while at the bottom it shows the harvesting efficiency ξ_i as a function of $\mathcal{P}_i$, as in (27). As we can observe, $\mathcal{G}(\mathcal{P}_i)$ saturates at $\mathcal{W} = 10.73$ mW when $\mathcal{P}_i \geq 14$ dBm, while it exhibits a maximal harvesting efficiency of $\xi_i = 73\%$ when $\mathcal{P}_i = 9$ dBm. Therefore, in order to maximize the

TABLE 3. Simulation parameters.

Description	Value
EH saturation level	$\mathcal{W} = 10.73$ mW
EH unitless constants	$c_0 = 0.2308$ $c_1 = 5.365$
Drain efficiency of the PA	$\eta = 33\%$
Fixed power consumption	$P_{\text{circ}} = 1.33$ mW
Maximal transmission power	$P_{\text{max}}^{\text{tx}} = 3.3$ dBm
Transmit power of the PB	$P_{\text{b}} = 45$ dBm
Number of antennas at the PB	$M \in \{4, 8\}$ antennas
Distances	$d_{\text{wet}} = 3$ m $d_{\text{wit}} = 100$ m
LOS parameters	$\kappa_{\text{wet}} = 4$ dB $\kappa_{\text{wit}} = 2$ dB
Path-loss exponents	$\alpha_{\text{wet}} = \alpha_{\text{wit}} = 3$
Carrier frequencies	$f_{\text{wet}} = 915$ MHz $f_{\text{wit}} = 2.45$ GHz
Channel coherence time	$T_{\text{c}} = 10$ ms
Target outage probability	$\mathcal{O}^\star = 10^{-6}$
Maximum time deadline	$T_{\text{max}} = 10$ ms
Maximal number of replicas	$K_{\text{max}} = 10$
Maximum spectral efficiency	$R_{\text{max}} = 8$ bps/Hz
Noise figure	$N_{\text{f}} = 10$ dBm
Noise PSD	$N_0 = -204$ dB/Hz
Packet length	$N = 56$ bits
Bandwidth	$B = 100$ kHz

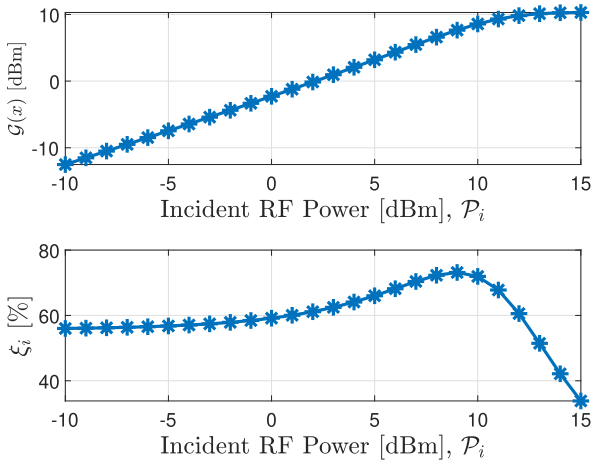

FIGURE 2. At the top: $\mathcal{G}(\mathcal{P}_i)$ as a function of $\mathcal{P}_i$. At the bottom: ξ_i as a function of $\mathcal{P}_i$.

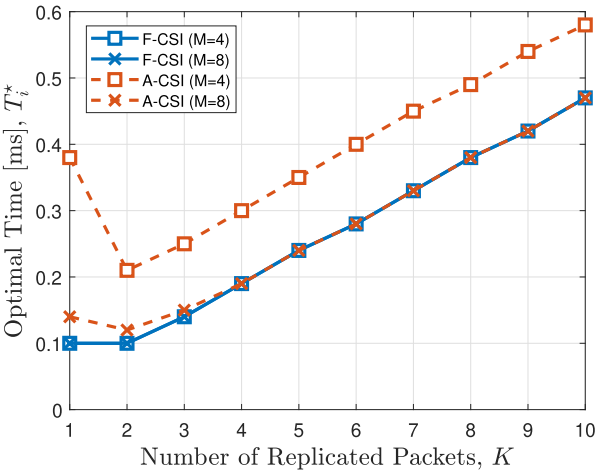

FIGURE 3. Optimal harvesting time $T_i^\star$ as a function of the number of replicated packets K in the WIT link.

energy efficiency one should operate below the saturation level, so that energy is not wasted, and as close as possible to the point of maximal ξ_i. In our scenario, $\mathcal{P}_i$ depends on the transmission scheme (A-CSI or F-CSI), but it can be roughly approximated using P_{b}, the average power gain of the WET link, and the beamforming gain due to the M antennas, so that $P_{\text{b}} = 45$ dBm yields $\mathcal{P}_i \approx 9$ dBm when $M = 4$ antennas, *i.e.*, exactly at the point of maximal energy efficiency of Figure 2. Therefore, our strategy focuses on maximizing the energy efficiency by optimizing T_i for a fixed P_{b}.

Figure 3 plots the optimal time $T_i^\star$ as a function of the number of replicated packets K. Notice that the minimal energy $\mathcal{E}_i^\star$ used by the PB can be directly inferred from Figure 3, since $\mathcal{E}_i^\star = P_{\text{b}} T_i^\star$. As we observe, there is an optimal pair $(K_i^\star, T_i^\star)$ that minimizes $\mathcal{E}_i^\star$. Comparing A-CSI with the F-CSI benchmark, we observe that $T_{\text{A-CSI}}^\star$ is larger than $T_{\text{F-CSI}}^\star$, but still lower than T_{max}, enabling industrial MTC applications [2]. Also, for both schemes we observe that PR is important to reduce the energy required by the PB, since $K_i^\star > 1$ in all the considered configurations. The results for F-CSI with $M = 4$ being very similar as with $M = 8$ are explained by the fact that F-CSI with $M = 4$ is already able to provide $P_{\text{F-CSI}}^{\text{tx}} = 3.3$ dBm, which is the maximal transmission power allowed by the BLE transceiver in [29]. Therefore, there is no need to increase the number of antennas at the PB in this case. Nevertheless, this is not the case for A-CSI, which benefits from increasing the number of antennas at the PB and approaches the performance of F-CSI when $M = 8$.

Figure 4 shows the optimal $T_i^\star$ that minimizes the energy required by the PB for different outage probability constraints, which is complemented by Figure 5 showing the optimal $K_i^\star$ that minimizes the energy required by the PB for different $\mathcal{O}^\star$. We observe that with lower $\mathcal{O}^\star$, both $K_i^\star$ and $T_i^\star$ must increase in order to meet the strict reliability constraints. The optimal $K_i^\star$ and $T_i^\star$ can be decreased if a larger number of antennas is employed at the PB, which improves the energy beamforming performance. Furthermore, we observe that $(K_{\text{A-CSI}}^\star, T_{\text{A-CSI}}^\star)$ is larger than $(K_{\text{F-CSI}}^\star, T_{\text{F-CSI}}^\star)$, with the gap increasing when $\mathcal{O}^\star$ decreases. Nevertheless, this is expected since we are considering an ideal F-CSI beamforming that serves only as a performance benchmark. Interestingly, the practical A-CSI beamforming still enables MTC applications.

Next, Figure 6 illustrates the minimal energy $\mathcal{E}_i^\star$ required by the PB as a function of the LOS factor κ_{wet} in the

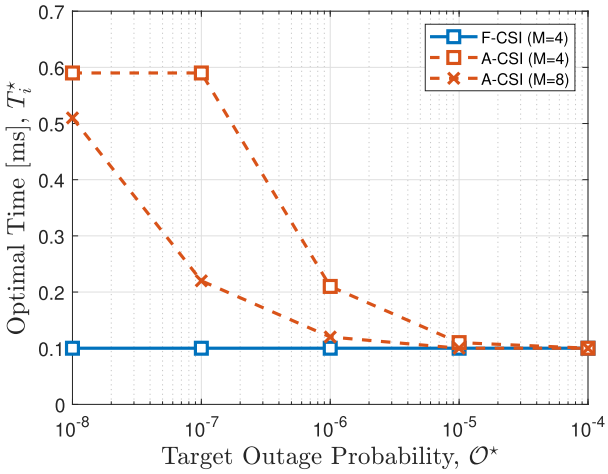

FIGURE 4. Optimal $T_i^\star$ that minimizes $\mathcal{E}_i^\star$, the energy required by the PB, for different target outage probabilities $\mathcal{O}^\star$.

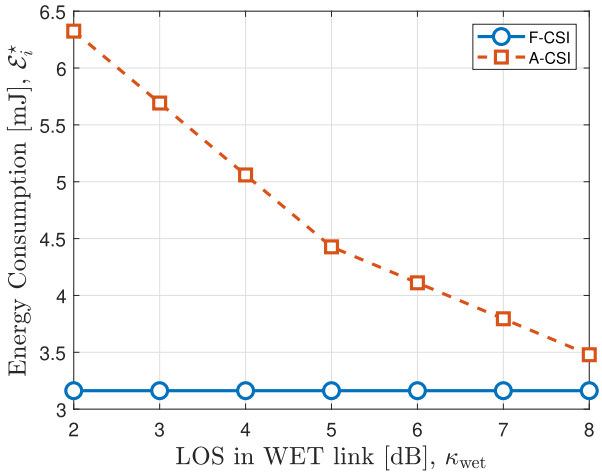

FIGURE 6. Minimal energy $\mathcal{E}_i^\star$ required by the PB for different LOS factors in the WET link κ_{wet}.

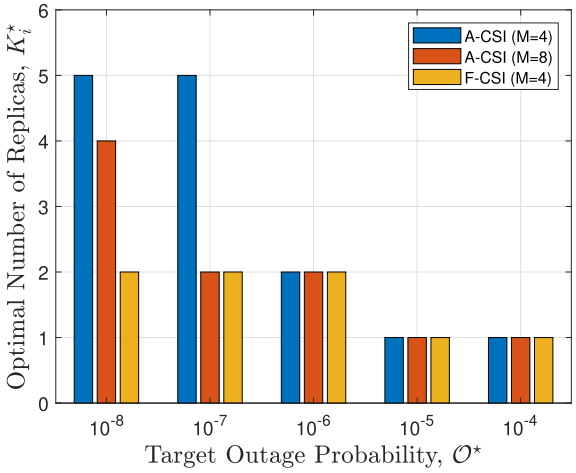

FIGURE 5. Optimal $K_i^\star$ that minimizes the energy $\mathcal{E}_i^\star$ required by the PB for different target outage probabilities $\mathcal{O}^\star$.

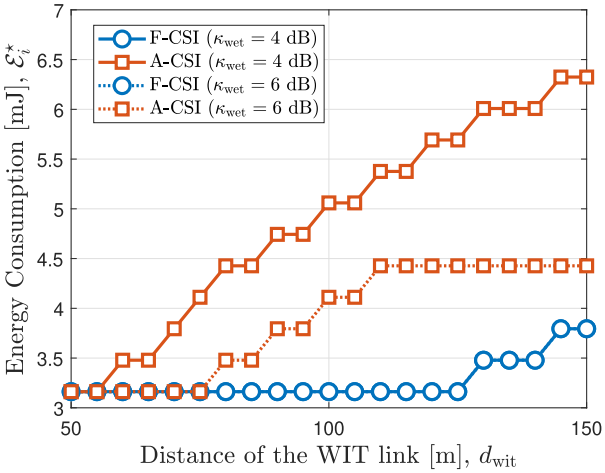

FIGURE 7. Minimal energy $\mathcal{E}_i^\star$ required by the PB as a function of the distance between source and destination d_{wit}.

WET link. Here we consider A-CSI and F-CSI schemes with $M = 8$ antennas and $\mathcal{O}^\star = 10^{-6}$. As we observe, the gap between both schemes decreases considerably when κ_{wet} increases. For example, $\mathcal{E}^\star_{\text{A-CSI}}$ is 100% higher than $\mathcal{E}^\star_{\text{F-CSI}}$ when $\kappa_{\text{wet}} = 2$ dB, while this gap drops to 60% when $\kappa_{\text{wet}} = 4$ dB and 10% when $\kappa_{\text{wet}} = 8$ dB. Such observation highlights that A-CSI is a viable beamforming option, especially if the PB can be positioned in a favorable condition, with strong LOS with respect to the source node.

Finally, Figure 7 plots $\mathcal{E}_i^\star$ as a function of the distance between source and destination nodes, d_{wit}. We consider A-CSI and F-CSI schemes with $M = 8$ antennas, $\mathcal{O}^\star = 10^{-6}$ and $\kappa_{\text{wet}} \in \{4, 6\}$ dB. Corroborating with Figure 6, F-CSI exhibits the same performance for both considered κ_{wet}. Comparing A-CSI and F-CSI beamforming, we notice very similar performance when d_{wit} is small. For instance, $\mathcal{E}^\star_{\text{A-CSI}}$ is 40% higher than $\mathcal{E}^\star_{\text{F-CSI}}$ when $d_{\text{wit}} = 80$ m with $\kappa_{\text{wet}} = 4$ dB, which is a typical transmission range of the considered BLE transceiver. Nevertheless, Figure 7 also shows that the increase in the energy consumption of A-CSI with d_{wit} can be mitigated by positioning the PB in a favorable condition. For instance, $\mathcal{E}^\star_{\text{A-CSI}}$ is 10% higher than $\mathcal{E}^\star_{\text{F-CSI}}$ at $d_{\text{wit}} = 80$ m with $\kappa_{\text{wet}} = 6$ dB, reinforcing the importance of a strong LOS with respect to the source node.

VI. CONCLUSION

This paper considered a batteryless MTC scenario with a dedicated multi-antenna PB to power the source node using A-CSI beamforming. The energy recovered at the source is used by the transceiver without storing it on a battery, since the charging time is typically in the order of a few seconds. That is a relevant issue often overlooked in the WET literature, and very relevant in MTC. Then, we derived the incident power statistics and the outage probability, assuming that the source employs PR in the WIT link to the destination. We formulated an iterative optimization algorithm in order to minimize the power consumed by the PB subject to stringent reliability constraints in the WIT link. The numerical results

showed the existence of an optimal harvesting time, as well as an optimal number of packet replications given the number of PB antennas. More importantly, the proposed scheme combining average CSI and packet replication was able to meet both the reliability and latency constraints of typical industrial MTC applications.

ACKNOWLEDGMENT

Rafaela Scaciota gratefully acknowledges the support of Onel L. Alcaraz López, the computer resources, and technical support provided by CWC.

REFERENCES

[1] Ericsson. (2022). *Ericsson Mobility Visualizer*. [Online]. Available: https://www.ericsson.com/en/reports-and-papers/mobility-report/mobility-visualizer

[2] J. Sachs, G. Wikstrom, T. Dudda, R. Baldemair, and K. Kittichokechai, "5G radio network design for ultra-reliable low-latency communication," *IEEE Netw.*, vol. 32, no. 2, pp. 24–31, Mar. 2018.

[3] B. Felix, I. Steuck, A. Santos, S. Secci, and M. Nogueira, "Redundant packet scheduling by uncorrelated paths in heterogeneous wireless networks," in *Proc. IEEE Symp. Comput. Commun. (ISCC)*, Jun. 2018, pp. 498–503.

[4] R.-A. Koutsiamanis, G. Z. Papadopoulos, T. L. Jenschke, P. Thubert, and N. Montavont, "Meet the PAREO functions: Towards reliable and available wireless networks," in *Proc. IEEE Int. Conf. Commun. (ICC)*, Jun. 2020, pp. 1–7.

[5] B. Chang, G. Zhao, L. Zhang, M. A. Imran, Z. Chen, and L. Li, "Dynamic communication QoS design for real-time wireless control systems," *IEEE Sensors J.*, vol. 20, no. 6, pp. 3005–3015, Mar. 2020.

[6] V. Kotsiou, G. Z. Papadopoulos, P. Chatzimisios, and F. Theoleyre, "LDSF: Low-latency distributed scheduling function for industrial Internet of Things," *IEEE Internet Things J.*, vol. 7, no. 9, pp. 8688–8699, Sep. 2020.

[7] P. Tuset-Peiro, F. Adelantado, X. Vilajosana, and R. D. Gomes, "Reliability through modulation diversity: Can combining multiple IEEE 802.15.4–2015 SUN modulations improve PDR?" in *Proc. IEEE Symp. Comput. Commun. (ISCC)*, Jul. 2020, pp. 1–6.

[8] D. D. Wolff, "The future of the IoT (batteries not required)," MIT News, Massachussets Int. Technol., Cambridge, MA, USA, Tech. Rep., 2021. [Online]. Available: https://news.mit.edu/2021/future-iot-batteries-not-required-0521

[9] O. L. A. Lopez, H. Alves, R. D. Souza, S. Montejo-Sánchez, E. M. G. Fernández, and M. Latva-Aho, "Massive wireless energy transfer: Enabling sustainable IoT toward 6G era," *IEEE Internet Things J.*, vol. 8, no. 11, pp. 8816–8835, Jun. 2021.

[10] F. A. Monteiro, O. L. A. Lopez, and H. Alves, "Massive wireless energy transfer with statistical CSI beamforming," *IEEE J. Sel. Topics Signal Process.*, vol. 15, no. 5, pp. 1169–1184, Aug. 2021.

[11] B. Clerckx, J. Kim, K. W. Choi, and D. I. Kim, "Foundations of wireless information and power transfer: Theory, prototypes, and experiments," *Proc. IEEE*, vol. 110, no. 1, pp. 8–30, Jan. 2022.

[12] Z. Mohamed and S. Aissa, "Coordinated energy beamforming: Wireless power coverage and transmission probability," in *Proc. IEEE Wireless Commun. Netw. Conf. (WCNC)*, Mar. 2021, pp. 1–6.

[13] Y. Ye, L. Shi, R. Q. Hu, and G. Lu, "Energy-efficient resource allocation for wirelessly powered backscatter communications," *IEEE Commun. Lett.*, vol. 23, no. 8, pp. 1418–1422, Aug. 2019.

[14] W. Ma, W. Wang, and T. Jiang, "Joint energy harvest and information transfer for energy beamforming in backscatter multiuser networks," *IEEE Trans. Commun.*, vol. 69, no. 2, pp. 1317–1328, Feb. 2021.

[15] O. M. Rosabal, O. L. A. Lopez, H. Alves, S. Montejo-Sanchez, and M. Latva-Aho, "On the optimal deployment of power beacons for massive wireless energy transfer," *IEEE Internet Things J.*, vol. 8, no. 13, pp. 10531–10542, Jul. 2021.

[16] Powercast. (2016). *P2110B-915 MHz RF Powerharvester Receiver*. [Online]. Available: http://www.powercastco.com/wp-content/uploads/2016/12/P2110B-Datasheet-Rev-3.pdf

[17] X. Yue, J. Kiely, D. Gibson, and E. M. Drakakis, "Charge-based supercapacitor storage estimation for indoor sub-mW photovoltaic energy harvesting powered wireless sensor nodes," *IEEE Trans. Ind. Electron.*, vol. 67, no. 3, pp. 2411–2421, Mar. 2020.

[18] Powercast. (2019). *P1110-EVAL-PS—PowerSpot RF Wireless Power Development Kit for Battery Recharging*. [Online]. Available: http://www.powercastco.com/wp-content/uploads/2019/04/PowerSpot-EVAL-01-User-Manual.V1.91.pdf

[19] B. Clerckx, R. Zhang, R. Schober, D. W. K. Ng, D. I. Kim, and H. V. Poor, "Fundamentals of wireless information and power transfer: From RF energy harvester models to signal and system designs," *IEEE J. Sel. Areas Commun.*, vol. 37, no. 1, pp. 4–33, Jan. 2019.

[20] O. L. A. Lopez, F. A. Monteiro, H. Alves, R. Zhang, and M. Latva-Aho, "A low-complexity beamforming design for multiuser wireless energy transfer," *IEEE Wireless Commun. Lett.*, vol. 10, no. 1, pp. 58–62, Jan. 2021.

[21] J. G. Proakis, *Digital Communications*. New York, NY, USA: McGraw-Hill, 2001.

[22] *Bluetooth Core Specification*, Bluetooth Core Specification Working Group, Version 5.3. 2021.

[23] C. Tellambura, A. J. Mueller, and V. K. Bhargawa, "Analysis of M-ary phase-shift keying with diversity reception for land-mobile satellite channels," *IEEE Trans. Veh. Technol.*, vol. 46, no. 4, pp. 910–922, Nov. 1997.

[24] S. Cui, A. J. Goldsmith, and A. Bahai, "Energy-efficiency of MIMO and cooperative MIMO techniques in sensor networks," *IEEE J. Sel. Areas Commun.*, vol. 22, no. 6, pp. 1089–1098, Aug. 2004.

[25] A. Goldsmith, *Wireless Communications*. 1st ed. Cambridge, U.K.: Cambridge Univ. Press, 2005.

[26] P. Mary, J.-M. Gorce, A. Unsal, and H. V. Poor, "Finite blocklength information theory: What is the practical impact on wireless communications?" in *Proc. IEEE Globecom Workshops (GC Wkshps)*, Dec. 2016, pp. 1–6.

[27] A. Gil, J. Segura, and N. M. Temme, "The asymptotic and numerical inversion of the Marcum Q-function," *Stud. Appl. Math.*, vol. 133, no. 2, pp. 257–278, Aug. 2014.

[28] W. H. Press, S. A. Teukolsky, W. T. Vetterling, and B. P. Flannery, *Numerical Recipes 3rd Edition: The Art of Scientific Computing*, 3rd ed. Cambridge, U.K.: Cambridge Univ. Press, 2007.

[29] M. Tamura, H. Takano, H. Nakahara, H. Fujita, N. Arisaka, S. Shinke, N. Suzuki, Y. Nakada, Y. Shinohe, S. Etou, T. Fujiwara, F. Kondo, K. Yamamoto, T. Matsumoto, and Y. Katayama, "A 0.5-V BLE transceiver with a 1.9-mW RX achieving −96.4-dBm sensitivity and −27-dBm tolerance for intermodulation from interferers at 6- and 12-MHz offsets," *IEEE J. Solid-State Circuits*, vol. 55, no. 12, pp. 3376–3386, Dec. 2020.

[30] S. Baek, D. Kim, M. Tesanovic, and A. Agiwal, "3GPP new radio release 16: Evolution of 5G for industrial Internet of Things," *IEEE Commun. Mag.*, vol. 59, no. 1, pp. 41–47, Jan. 2021.

RAFAELA SCACIOTA (Student Member, IEEE) was born in São Paulo, Brazil. She received the B.Sc. the Ph.D. degrees in electrical engineering from the Federal University of Technology-Paraná (UTFPR), Curitiba, Brazil, in 2018 and in 2022, respectively. From November 2021 to December 2021, and February 2022 to April 2022, she was a Visiting Researcher with the Centre of Wireless Communication, University of Oulu, Finland. Since May 2022, she has been with the University of Oulu, where she is currently a Postdoctoral Researcher. Her research interests include networked control systems, wireless communications, energy efficiency, and energy harvesting.

ONEL L. ALCARAZ LÓPEZ (Member, IEEE) received the B.Sc. (Hons.), M.Sc., and D.Sc. (Hons.) degrees in electrical engineering from the Central University of Las Villas (Cuba), the Federal University of Paraná (Brazil), and the University of Oulu (Finland), respectively. From 2013 to 2015, he served as a Specialist in telematics with Cuban Telecommunications Company (ETECSA). He currently holds an Assistant Professorship (tenure track) in sustainable wireless communications engineering with the Centre for Wireless Communications (CWC), Oulu, Finland. He is coauthor of the book titled *Wireless RF Energy Transfer in the Massive IoT Era: Towards Sustainable Zero-Energy Networks* (Wiley), in December 2021. His research interests include sustainable IoT, energy harvesting, wireless RF energy transfer, wireless connectivity, and machine-type communications. He is a Collaborator to the 2016 Research Award given by the Cuban Academy of Sciences, a co-recipient of the 2019 IEEE EuCNC Best Student Paper Award, and the author of the Best Doctoral Thesis in engineering, Finland, in 2020.

GLAUBER BRANTE (Senior Member, IEEE) received the Ph.D. degree in electrical engineering from the Federal University of Technology—Paraná (UTFPR), Curitiba, Brazil, in 2013. In 2012, he was a Visiting Researcher with the Institute of Information and Communication Technologies, Electronics, and Applied Mathematics, Catholic University of Louvain, Belgium. He is currently an Assistant Professor with UTFPR. His research interests include wireless communications, machine-type communications, energy efficiency, and energy harvesting. He was a recipient of the Best Ph.D. Thesis Award in electrical engineering, Brazil, in 2014. He was a co-recipient of the 2016 Research Award from the Cuban Academy of Sciences. He was Co-Editor-in-Chief for the *Journal of Communication and Information Systems*, from 2018 to 2020. Since 2018, he has been serving as an Associate Editor for the IEEE COMMUNICATIONS LETTERS, since 2019 he has been serving as an Associate Editor for the IEEE OPEN JOURNAL OF THE COMMUNICATIONS SOCIETY, and since 2022 he has been serving as an Associate Editor for the IEEE WIRELESS COMMUNICATIONS LETTERS.

RICHARD DEMO SOUZA (Senior Member, IEEE) received the D.Sc. degree in electrical engineering from the Federal University of Santa Catarina (UFSC), Brazil, in 2003. From 2004 to 2016, he was with the Federal University of Technology—Paraná (UTFPR), Brazil. Since 2017, he has been with UFSC, where he is a Professor. His research interests include wireless communications and signal processing. He is a co-recipient of the 2014 IEEE/IFIP Wireless Days Conference Best Paper Award, the Supervisor of the awarded Best Ph.D. Thesis in electrical engineering, Brazil, in 2014, and a co-recipient of the 2016 Research Award from the Cuban Academy of Sciences. He has served as Editor or Associate Editor for the *SBrT Journal of Communications and Information Systems*, the IEEE COMMUNICATIONS LETTERS, the IEEE TRANSACTIONS ON VEHICULAR TECHNOLOGY, the IEEE TRANSACTIONS ON COMMUNICATIONS, and the IEEE INTERNET OF THINGS JOURNAL.

ANDRÉ A. MARIANO (Senior Member, IEEE) received the B.S. degree in electrical engineering from the Federal University of Paraná (UFPR), Curitiba, Paraná, Brazil, in 2002, and the M.S. degree in microelectronics and the Ph.D. degree in electronics from the University of Bordeaux, Bordeaux Cedex, France, in 2004 and 2008, respectively. From 2004 to 2010, he was with the STMicroelectronics-IMS Joint Research Laboratory, IC Design Team. He developed a high-speed continuous-time delta-sigma A/D converter dedicated to software-defined radio and front-end receiver building blocks for millimeter-wave applications (from 60 to 77 GHz). Since February 2011, he has been an Associate Professor with the Department of Electrical Engineering, UFPR, and a member of the Group of Integrated Circuits and Systems (GICS). He has several publications in journals, international and national conferences, and holds one patent. His research interests include design of RFICs and high-speed mixed ICs. He is a member of the Group of Integrated Circuits and Systems (GICS) and also a member of the Technical Program Committees of the IEEE Latin American Symposium on Circuits and Systems (LASCAS) and Symposium on Integrated Circuits and Systems Design (SBCCI).

GUILHERME LUIZ MORITZ (Member, IEEE) was born in Gaspar, Brazil, in 1984. He received the B.Sc. and D.Sc. degrees in electrical engineering from the Federal University of Technology—Paraná (UTFPR), Curitiba, Brazil, in 2012 and 2015, respectively, where he is currently an Assistant Professor of embedded systems, control systems, and wireless sensor networks. His research interests include wireless communications, cooperative communications, and the Internet of Things.